ELSEVIER

Journal of Nuclear Materials 318 (2003) 292–299

journal of nuclear materials

www.elsevier.com/locate/jnucmat

Tensile properties of Inconel 718 after low temperature neutron irradiation

T.S. Byun *, K. Farrell

Metal and Ceramics Division, Oak Ridge National Laboratory, Building 5500, P.O. Box 2008, MS-6151, Oak Ridge, TN 37831, USA

Abstract

Tensile properties of Inconel 718 (IN718) have been investigated after neutron irradiation to 0.0006–1.2 dpa at 60–100 °C in the High Flux Isotope Reactor (HFIR) at Oak Ridge National Laboratory (ORNL). The alloy was exposed in solution-annealed (SA) and precipitation-hardened (PH) conditions. Before irradiation, the yield strength of PH IN718 was about 1170 MPa, which was 3.7 times higher than that of SA IN718. In the SA condition, an almost threefold increase in yield strength was found at 1.2 dpa, but the alloy retained a positive strain-hardening capability and a uniform ductility of more than 20%. Comparisons showed that the strain-hardening behavior of the SA IN718 is similar to that of a SA 316LN austenitic stainless steel. In the PH condition, the IN718 displayed no radiation-induced hardening in yield strength and significant softening in ultimate tensile strength. The strain-hardening capability of the PH IN718 decreased with dose as the radiation-induced dissolution of precipitates occurred, which resulted in the onset of plastic instability at strains less than 1% after irradiation to 0.16 or 1.2 dpa. An analysis on plastic instability indicated that the loss of uniform ductility in PH IN718 was largely due to the reduction in strain-hardening rate, while in SA IN718 and SA 316LN stainless steel it resulted primarily from the increase of yield stress.

1. Introduction

Inconel 718 alloy is a precipitation hardenable, nickel-based superalloy which has decent corrosion resistance, high strength at ambient temperature, and excellent creep and fatigue strengths at high temperature. Thus the alloy has been used for a variety of applications such as gas turbines, jet engines, steam generators, and fission and fusion reactor structures [1–10]. Recently, the alloy has been used for the beam window and other components of the Los Alamos Neutron Science Center (LANSCE) accelerator, and was selected as a back-up material for target components of the Spallation Neutron Source (SNS) under construction at Oak Ridge National Laboratory (ORNL) and other large-scale accelerators [11–16]. In those applications, the alloy has a composite structure of austenitic matrix and precipitated γ' and γ'' phases produced by a typical heat treatment consisting of solution annealing and aging [17]. It is known that high fluence irradiation of this composite structure undergoes negligible radiation-induced hardening or even softening with considerable decrease in ductility [7,11–13]. Transmission electron microscopy (TEM) investigations [4,15,16] show that superlattice spots diffracted from the γ' and γ'' precipitates disappeared from the diffraction patterns of the aged Inconel 718 after irradiation to a fraction of 1 dpa. The dose-dependent softening was explained by the radiation-induced dissolution of the hard precipitates [13–16].

Although the low-temperature irradiation response of solution-annealed IN718 is unknown [16], it is expected to behave like other solution-annealed face-centered cubic (f.c.c) materials such as 304 and 316 stainless steels [18–21], which usually demonstrate significant radiation-induced hardening and retain high strain-hardening capability after irradiation. In the IN718 alloy, if the aging process for precipitate hardening is omitted in the heat treatment [1], radiation-induced softening might

* Corresponding author. Tel.: +1-865 576 7738; fax: +1-865 574 0641.

E-mail address: byunts@ornl.gov (T.S. Byun).

0022-3115/03/$ - see front matter
doi:10.1016/S0022-3115(03)00006-0

not occur and better ductility might be achieved. Thus, it is proposed that the IN718 alloy in a SA condition might be useful in nuclear applications where the strength of the material is not a critical service factor. The present experiment was designed to elucidate the effect of two different initial microstructural conditions on the mechanical properties of the IN718 alloy after irradiation. Tensile specimens with and without the γ' and γ'' precipitates were irradiated up to 1.2 dpa at 60–100 °C and tested at room temperature. The strain-hardening properties of SA and PH Inconel 718 are analyzed and compared with those of 316LN stainless steel [18,19].

2. Experimental

The material studied was the nickel base alloy 718 in the precipitation-hardened and solution-annealed conditions. The chemical composition of the alloy was, in wt%, 18.3Fe, 18.13Cr, 5.07Nb, 3.0Mo, 1.1Ti, 0.54Al, 0.4Co, 0.21Mn, 0.13Si, 0.05C with the balance Ni. Flat tensile specimens of nominal gage section dimensions of 0.76 mm thick, 1.5 mm wide and 7.6 mm long were cut from sheet material in the rolling direction. Complete dimensions of the specimens are given in Fig. 1. Machining and sanding operations were completed before the specimens were heat-treated. All specimens were solution-annealed in vacuum at 1065 °C for 30 min. Then, some SA specimens were aged, or precipitation-hardened, at 750 °C for 10 h followed by 20 h at 650 °C to form γ' and γ'' precipitates in the austenitic matrix.

Irradiation of the specimens was carried out in the hydraulic tube facility of the HFIR. The bare specimens were in direct contact with rapidly flowing water coolant and their temperature was estimated to be in the range 60–100 °C. The fluences of fast neutron ($E > 1$ MeV) ranged from 3.7×10^{21} to 7.8×10^{24} n m^{-2}. Corresponding nominal displacements per atom (dpa) levels were estimated to range from 0.00057 to 1.2 dpa. The irradiation conditions for tensile specimens are summarized in Table 1.

All tensile tests were conducted at room temperature in a screw-driven machine at a crosshead speed of 0.008 mm s^{-1}, corresponding to a strain rate of approximately 1×10^{-3} s^{-1}. Strains were calculated from the recorded crosshead separation using an initial nominal gauge length of 7.62 mm. Engineering stress and true stress were calculated as the applied load divided by the initial cross sectional area, A_0, and by the reduced cross sectional area during deformation, $A_0 \exp(-\varepsilon_p)$, respectively. The true plastic strain, ε_p, is derived from the plastic elongation, e_p, as $\varepsilon_p = \ln(1 + e_p)$.

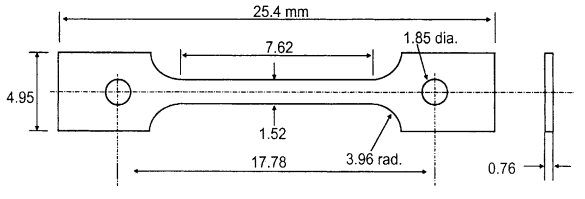

Fig. 1. Dimensions of SS-3 tensile specimen.

3. Results and discussion

3.1. Tensile properties

The engineering tensile test curves of IN718 alloy in PH and SA conditions are shown in Figs. 2 and 3, respectively. In Fig. 2, the engineering stresses of the PH IN718 are high and are not strongly affected by irradiation. There is progressive reduction in elongation with increasing dose. In the dose range 0–0.054 dpa, the material retained positive strain-hardening rate until plastic strain reached 9% or more. At higher doses the specimens showed short strain hardening in early deformation but started to deform in an instable mode at small plastic strains of about 1.5%.

In Fig. 3, the SA IN718 is much weaker than the PH IN718 and it shows larger fractional increase in radiation-induced strengthening. Small yield drops and/or short plateaus are present at yield in the stress–strain curves after irradiation. Unlike the PH IN718, the SA IN718 retained high elongation after irradiation; the uniform elongation was more than 20% at the highest dose of 1.2 dpa. Such significant ductility after irradiation was also found in other annealed f.c.c. metals such as austenitic stainless steels [18–21]. At room temperature the austenitic stainless steels retained more than 20% uniform elongation after irradiation to 1 dpa, and even at 11 dpa the steels displayed significant uniform ductility up to 12% [18–21].

The strength and ductility parameters for the two microstructural conditions are extracted from the tensile curves and compared as functions of dpa in Figs. 4 and 5. As displayed in Fig. 4, neutron irradiation barely changed the yield strength of the PH IN718, while the yield strength of the SA alloy increased strongly with dose, and at the highest dose of 1.2 dpa it reached about 2.7 times higher than that of the unirradiated condition. With regard to their ultimate strengths, the SA IN718 showed moderate radiation-induced hardening, while the PH IN718 experienced radiation-induced softening. For the SA IN718, the strengthening after significant plastic deformation was moderate; the ultimate tensile strength was only 20% higher than that of the unirradiated material. This increase is notably lower than the respectable 170% increase in the yield strength. Another sharp contrast between the PH and SA conditions can be seen in the ratio of ultimate tensile strength to yield strength. Before irradiation, the ratios were very

Table 1
Radiation doses for tensile specimens

Specimen ID	Heat treatment	HFIR rabbit ID	Fluence (10^{24} n m^{-2}, $E > 1$ MeV)	dpa
N29	Aged	Control	0.0	0.0
N30	Aged	Control	0.0	0.0
N18	Aged	8-97-4	0.0037	0.00057
N19	Aged	8-97-4	0.0037	0.00057
N20	Aged	8-97-3	0.022	0.0034
N21	Aged	8-97-3	0.022	0.0034
N22	Aged	8-97-2	0.096	0.015
N23	Aged	8-97-2	0.096	0.015
N24	Aged	8-97-1	0.35	0.054
N25	Aged	8-97-1	0.35	0.054
N26	Aged	5-98-6	1.06	0.16
N28	Aged	7-98-2	8.30	1.2
N12	Annealed	Control	0.0	0.0
N13	Annealed	Control	0.0	0.0
N1	Annealed	8-97-4	0.0037	0.00057
N2	Annealed	8-97-4	0.0037	0.00057
N3	Annealed	8-97-3	0.022	0.0034
N4	Annealed	8-97-3	0.022	0.0034
N5	Annealed	8-97-2	0.096	0.015
N6	Annealed	8-97-2	0.096	0.015
N7	Annealed	8-97-1	0.35	0.054
N8	Annealed	8-97-1	0.35	0.054
N9	Annealed	5-98-6	1.06	0.16
N11	Annealed	7-98-2	8.30	1.2

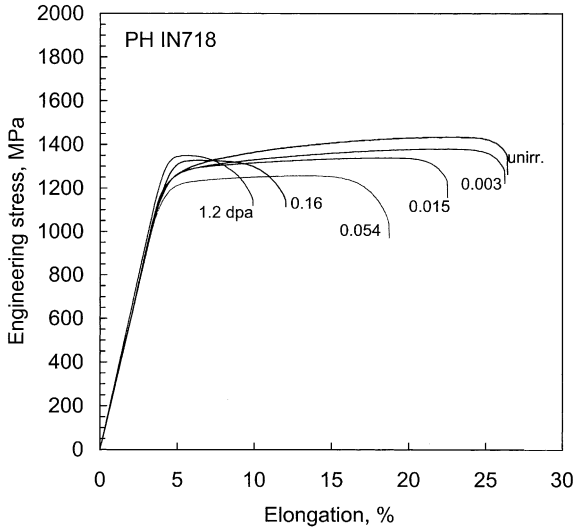

Fig. 2. Engineering stress–strain curves of precipitation-hardened IN718 at various doses.

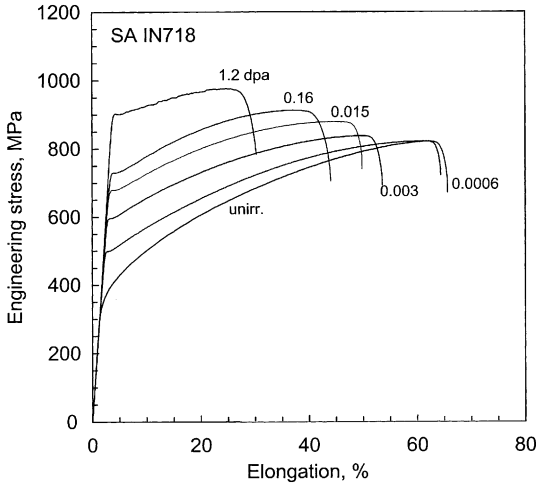

Fig. 3. Engineering stress–strain curves of solution-annealed IN718 at various doses.

different: 1.2 and 2.5 for the PH and SA conditions, respectively. After irradiation, however, both conditions gave reduced values of about 1.1.

The variations of uniform and total elongations are given in Fig. 5. The fractional loss of ductility due to irradiation was also quite different for the two conditions. Before irradiation, much lower elongation was measured in the PH IN718 than in the SA IN718. After irradiation to 1.2 dpa, the PH IN718 retained only a small uniform elongation of 1.5%, or less than 10% of its initial uniform ductility, while the SA IN718 retained

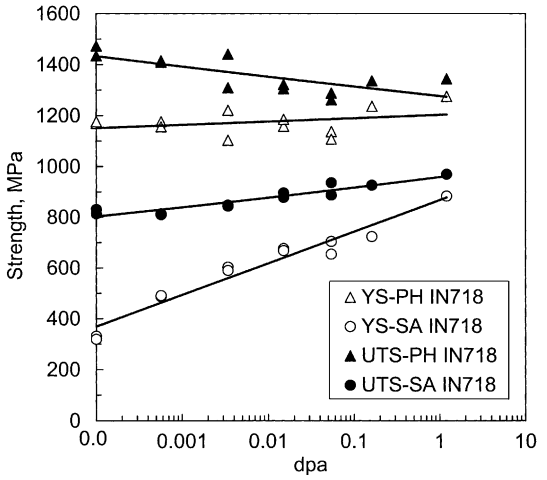

Fig. 4. Variations of yield and ultimate tensile strengths with dpa in PH and SA conditions.

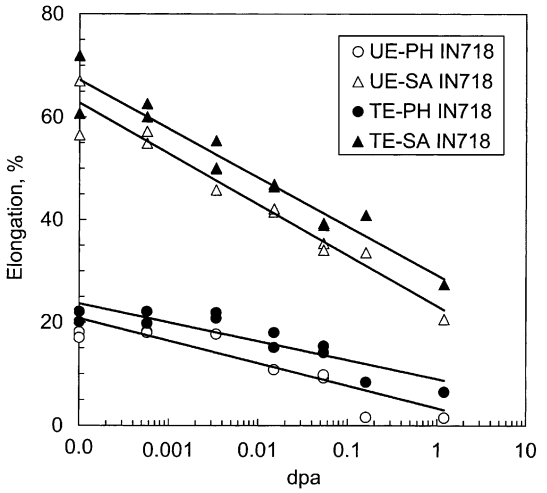

Fig. 5. Variations of uniform and total elongations with dpa in PH and SA conditions.

more than 20% uniform elongation, or more than 1/3 of initial ductility. The reductions in total elongation were significant for both PH and SA conditions, and again the PH IN718 showed the relatively larger reduction. For both conditions, the difference between uniform elongation and total elongation was nearly independent of dose.

3.2. True stress–true strain behaviors

Fig. 6 presents the true stress (σ)–true strain (ε) curves in the uniform deformation range calculated from the engineering stress–strain curves in Figs. 2 and 3. The slopes of the curves, strain-hardening rate ($d\sigma/d\varepsilon$), decreased as dose increased. After yield, or yield plateau for the annealed and irradiated specimens, the stress–strain curves showed positive strain hardening until a plastic instability occurred at the uniform deformation limit, which corresponds to the ultimate load.

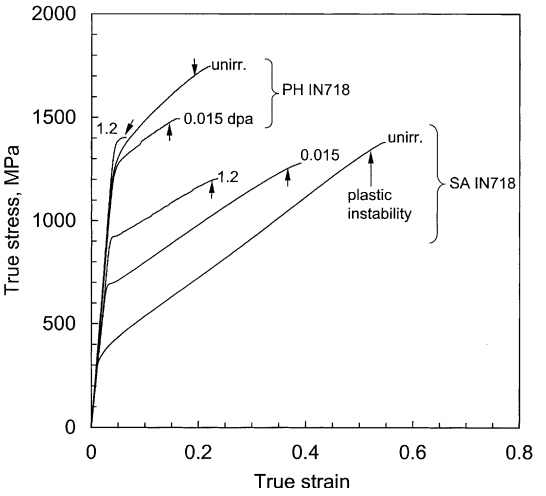

Fig. 6. True stress–true strain curves of IN718 alloy in PH and SA conditions.

The average strain-hardening rates were calculated over the uniform plastic strain range and are plotted as functions of dose in Fig. 7. In this figure the values for SA 316LN stainless steel, which was irradiated and tested in the same experiment package [22], are also included for comparison. Among the three materials, the PH IN718 showed the highest strain-hardening rates, 3000–3500 MPa before irradiation, however, its strain-hardening rate decreased most rapidly with increasing

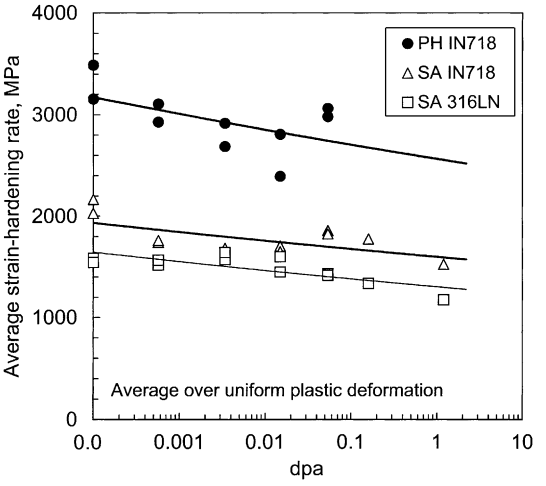

Fig. 7. Comparison of the dose dependences of average strain-hardening rate.

dose. In the SA condition 316LN stainless steel gave lower level of strain-hardening rate than IN 718, but similar dose dependencies were observed for the two alloys. In the dose range 0–1.2 dpa the strain-hardening rates were in the ranges 1500–2200 MPa for the SA IN718 and 1200–1800 MPa for the SA 316LN stainless steel.

In the curves in Fig. 6 it is noticed that irradiation reduced the slope of PH IN718 without significant change in the yield stress. In the SA IN718, however, irradiation increased the yield stress significantly with moderate change in the slope. In the Fig. 8 the plot of average strain-hardening rate against yield stress illustrates a clear contrast between the PH and SA conditions. In SA alloys the average strain-hardening rate decreased in a moderate pace as the yield stress increases, in the PH IN718, however, the average strain-hardening rate was nearly independent of the yield stress.

In Fig. 6 arrows indicate the onsets of plastic instabilities. Total strain-hardening capability can be measured by the difference between the yield stress and the instability stress, or the true stress at the onset of necking. From these two stress parameters, stress-dose diagrams were constructed for the three materials as seen in Fig. 9. In the SA alloys the yield stress increased rapidly with dose due to irradiation hardening while the instability stress was relatively insensitive to dose [19]. In the aged IN718, however, the yield stress is insensitive to dose as the plastic instability stress decreases with dose. According to Considere's criterion [23], when the yield stress exceeds the instability stress, a necking or plastic instability will occur at yield. As indicated in Fig. 9, necking at yield did not occur in any of the three materials in the dose range 0–1.2 dpa. But the dose to

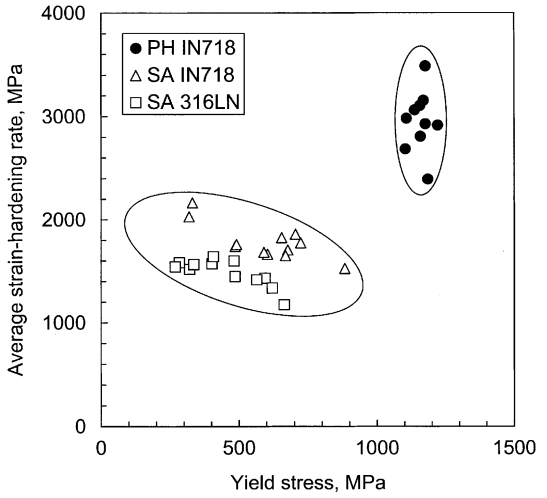

Fig. 8. Comparison of the yield stress dependences of average strain-hardening rate.

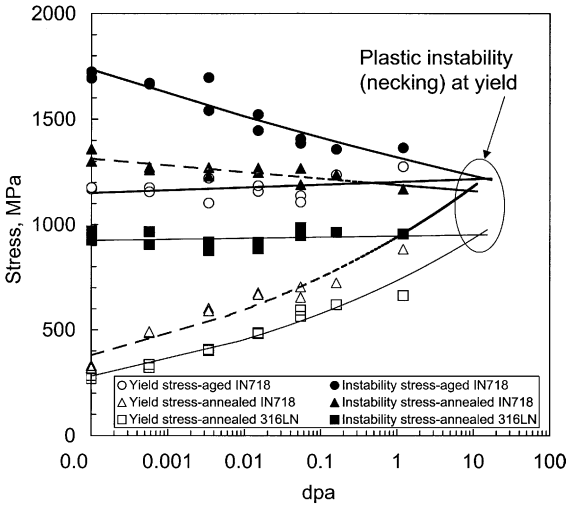

Fig. 9. Dose dependences of yield stress and instability stress and prediction of the dose to plastic instability at yield.

plastic instability at yield, the dpa value at which the yield stress equals plastic instability stress, can be predicted by extrapolation of the regression curves to a higher dpa range. An instability at yield will not occur until the dose reaches a critical value at which the extrapolated yield stress and plastic instability stress curves intersect. Regardless of the sharp differences in the mechanical properties of the annealed and aged conditions, the doses to plastic instability at yield were predicted at marginally close values: 8 dpa for SA IN718, 14 dpa for PH IN718 and 12 dpa for SA 316LN stainless steel.

For the PH IN718, this method to predict the dose to plastic instability at yield can carry an uncertainty since an excessive extrapolation may not be allowed if changes in precipitates during irradiation alter the trends of mechanical behavior abruptly. However, the predicted value, 14 dpa, seems reasonable considering the results for higher doses; the PH IN718 retained about 1% uniform plastic ductility at 10 dpa but showed a brittle failure at a stress below anticipated yield stress at 20 dpa [12]. Further, the predicted value for SA 316LN stainless steel, 12 dpa, agreed with the predicted value, 14 dpa, using the tensile test data after proton and neutron irradiation up to 11 dpa [19].

3.3. Uniform ductility as a function of yield stress and hardening rate

It is worth noting that the PH IN718, which has the highest strain-hardening rate among the three materials, shows much lower ductility than the two annealed alloys, as seen in Fig. 5. In general, a higher strain-hardening rate results in a higher ductility [23]. However, the high strength of PH IN718 seems to shorten the uniform

deformation, which results in a lower ductility. It is believed that the strength of a material, as well as the strain-hardening rate, is a key factor determining the uniform ductility. This has been also pointed out in a recent finite element analysis by Odette et al. [24].

Following Odette et al. [24], the influences of strength and strain hardening on the uniform ductility explored using a power-law strain hardening model, or Ludwik equation [23]:

$$\sigma(\varepsilon_p) = \sigma_y + h(\varepsilon_p)^m, \tag{1}$$

where σ_y is the yield stress, ε_p the true plastic strain, and h, m the hardening coefficient and exponent of the parabolic hardening term, respectively. In Eq. (1) the strain-independent term σ_y and strain-dependent hardening term $h(\varepsilon_p)^m$ are separated to explain the influences of radiation-induced strengthening and change in work-hardening rate on the uniform ductility. Applying Considere's condition for plastic instability,

$$\sigma = \left.\frac{d\sigma}{d\varepsilon_p}\right|_{\varepsilon_p=\varepsilon_p^u}, \tag{2}$$

to Eq. (1), an expression for uniform strain ε_p^u is given by

$$\sigma_y + h(\varepsilon_p^u)^m = hm(\varepsilon_p^u)^{m-1}. \tag{3}$$

To solve the Eq. (3) for uniform strain, the exponent m was measured over the uniform strain range of the true stress–true strain curves. These measured values of m were in a narrow range for each material; the average value was about 0.9 for the SA IN718 and about 0.6 for the PH IN718. The values for h, 500 and 1100 MPa for $m = 0.9$ and 400 and 1400 MPa for $m = 0.6$, were chosen so that the solution curves can bound the experimental data. Note that the values for h chosen for the calculation of uniform strains are lower than the measurements. The reason for not using the measurements for h is that using the measurements for both constants results in large errors in the predicted uniform strains. This also implies that the strain-hardening term determined by the two constants, h and m, is not accurate enough to describe the details of experimental flow curves of the test materials. Four solution curves, the uniform strain versus yield stress curves, from the pairs of coefficients, h and m, are plotted in Fig. 10. The tensile test data for the SA IN718, SA 316LN, and PH IN718 are also presented in Fig. 10 for comparison.

An important conclusion from the solutions of Eq. (3) is that the uniform strain can decrease with increasing yield stress without any change in hardening term. Especially, the uniform strain decreases rapidly in the low yield stress region, which predicts that an annealed material having an original low yield stress will show rapid reduction in uniform ductility as the material is strengthened by irradiation. An equally important conclusion is that the uniform strain of a material can be significantly reduced by a reduction in strain hardening even where there is little change in yield stress.

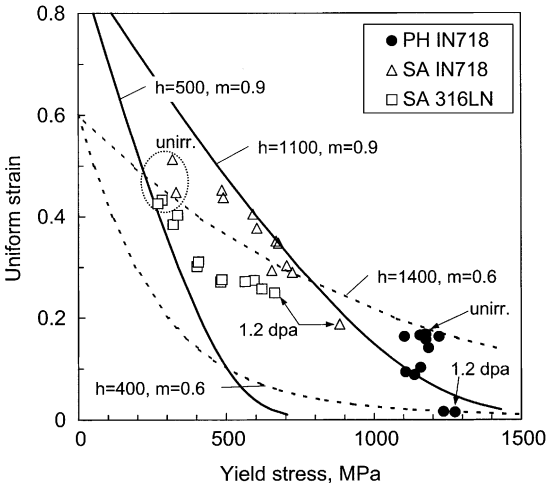

Fig. 10. Uniform strain versus yield stress curves with different strain hardening. Tensile test data for three austenitic materials are overlaid with the curves.

If the neutron irradiation increases the yield stress without changing the strain-hardening behavior, the yield stress and uniform strain data will be overlaid on a solution curve. In Fig. 10, however, the tensile test data do not follow a single solution curve but are better represented by different solution curves. In the PH IN718 the uniform strain decreased with radiation dose with little change in yield stress, which means that the uniform ductility of the PH IN718 decreased mainly due to the reduction in strain-hardening rate. Different pairs of h- and m-values must be used to describe the strain-hardening behaviors of the PH IN718 specimens irradiated to different doses. In the SA alloys, on the other hand, the neutron irradiation raises the yield stress and reduces the strain-hardening rate [19]. As indicated in Fig. 8, the yield stress increased with dose in a larger degree than the strain-hardening rate. This indicates that in the SA alloys the reduction in uniform strain seems to be caused more by the increase of yield stress than by the reduction of strain-hardening rate.

3.4. Microstructural changes and mechanical properties

No microstructure study was conducted in the present work. However, the origins of the large differences in the tensile properties of the IN718 alloy in its SA and PH conditions are undoubtedly determined by microstructure. The SA IN718 is a single phase, solid solution alloy. In the PH IN718, a high strength composite microstructure is developed during thermal aging by

precipitation of spheroidal γ' ($Ni_3(Ti,Al)$) and disk-shaped γ'' (Ni_3Nb) phases in the f.c.c. matrix [4,16]. The γ' and γ'' phases resist plastic flow, which produces high strength at ambient temperature as well as excellent creep rupture strength at high temperatures up to 700 °C [3,6]. These are susceptible to radiation-induced changes in structure, composition, and cohesion with the matrix [12–16]. Such changes alter the physical and mechanical properties of the phase and reduce its capability as a hardening agent.

The dissolution of the hard γ' and γ'' phases is recognized as an important phenomenon influencing the mechanical behavior of irradiated PH IN718 [11–16]. After irradiation to 0.1 dpa with protons and neutrons, the images of the γ' and γ'' phases lost some of their intensity and disordering occurred in the second phases [13–15]. At a dose of 0.6 dpa, all evidence of the γ' and γ'' precipitates disappeared from diffraction patterns, which was mainly due to a complete disordering in the γ' and γ'' phases. Softening from these phase changes was counterbalanced to a large extent by the generation of radiation-induced point defect clusters, with the net effect of little change in flow stress. The irradiated SA IN718 showed the typical defect structures of annealed and irradiated alloys [25]. The microstructural changes in both SA and PH IN718 alloys due to irradiation are discussed in detail in Ref. [25].

4. Summary and conclusions

Tensile properties of Inconel 718 alloy in SA and PH conditions have been investigated after low temperature neutron irradiation up to 1.2 dpa. The summary and conclusions drawn from the test and analysis results are as follows:

(1) In the SA IN718, an almost threefold increase in yield strength was found at 1.2 dpa and the material retained a strong strain-hardening capability and a high uniform ductility of more than 20%. However, the originally much stronger PH IN718 displayed little radiation-induced hardening in yield strength and significant softening in ultimate tensile strength.

(2) The strain-hardening behavior of the SA IN718 was shown to be similar to that of SA 316LN austenitic stainless steel and their average strain-hardening rate decreased slightly with dose. The IN718 in PH condition displayed much higher strain-hardening rates than in SA condition; however, it experienced larger deterioration of strain-hardening capability after irradiation.

(3) An analysis of correlation between the uniform ductility and the plastic flow curve parameters, the yield stress and strain-hardening rate, indicates that the uniform strain decreases with increasing yield stress as well as with deteriorating strain-hardening capability. In PH IN718 the uniform ductility decreased mainly due to the reduction in strain-hardening rate, while in the SA alloys the reduction in uniform ductility originated largely from the increase of yield stress.

Acknowledgements

This research was sponsored by the Spallation Neutron Source Project, Office of Science, US Department of Energy, under Contract DE-AC05-00OR22725 with UT-Battelle, LLC. We would like to thank Drs L.K. Mansur and J.D. Hunn for technical review of the manuscript.

References

[1] J.M. Pereira, B.A. Lerch, Int. J. Impact Eng. 25 (2001) 715.
[2] G. Pottlacher, H. Hosaeus, B. Wilthan, E. Kaschnitz, A. Seifter, Thermochim. Acta 382 (2002) 225.
[3] W.L. Mankins, S. Lamb, Metals Handbook, Nickel and Nickel Alloys, Vol. 2, 10th Ed., ASM International, 1990, p. 428.
[4] S.J. Hong, W.P. Chen, T.W. Wang, Metall. Mater. Trans. A 32 (2001) 1887.
[5] H. Andersson, C. Persson, T. Hansson, Int. J. Fatigue 23 (2001) 817.
[6] C.Y. Jo, D.W. Joo, I.B. Kim, Mater. Sci. Tech. 17 (2001) 1191.
[7] P.G. de Heij, D. d'Hulst, J. van Hoepen, E.V. van Osch, J.G. van der Laan, Fusion Eng. Des. 58&59 (2001) 775.
[8] G. Kalinin, V. Barabash, A. Cardella, J. Dietz, K. Ioki, R. Matera, R.T. Santoro, R. Tivey, J. Nucl. Mater. 283 (2000) 10.
[9] R. Scholz, R. Matera, J. Nucl. Mater. 283 (2000) 414.
[10] R. Scholz, R. Matera, Fusion Eng. Des. 51 (2000) 165.
[11] S.A. Maloy, M.R. James, G. Willcutt, W.F. Sommer, M. Sokolov, L.L. Snead, M.L. Hamilton, F. Garner, J. Nucl. Mater. 296 (2001) 119.
[12] M.R. James, S.A. Maloy, F.D. Gac, W.F. Sommer, J. Chen, H. Ullmaier, J. Nucl. Mater. 296 (2001) 139.
[13] F. Carsughi, D. Derz, P. Ferguson, G. Pott, W. Sommer, H. Ullmaier, J. Nucl. Mater. 264 (1999) 78.
[14] M. García-Mazarío, M. Hernández-Mayoral, A.M. Lancha, J. Nucl. Mater. 296 (2001) 192.
[15] B.H. Sencer, G.M. Bond, F.A. Garner, M.M. Hamilton, S.A. Maloy, W.F. Somer, J. Nucl. Mater. 296 (2001) 145.
[16] J.D. Hunn, E.H. Lee, T.S. Byun, L.K. Mansur, J. Nucl. Mater. 296 (2001) 2003.
[17] C. Slama, M. Abdellaoui, J. Alloys Compd. 306 (2000) 277.
[18] K. Farrell, T.S. Byun, J. Nucl. Mater. 296 (2001) 129.
[19] T.S. Byun, K. Farrell, E.H. Lee, J.D. Hunn, L.K. Mansur, J. Nucl. Mater. 298 (2001) 269.
[20] S.A. Maloy, M.R. James, G. Wilcutt, W.F. Sommer, M. Sokolov, L.L. Snead, M.L. Hamilton, F. Garner, J. Nucl. Mater. 296 (2001) 119.
[21] J.E. Pawel, A.F. Rowcliffe, G.E. Lucas, S.J. Zinkle, J. Nucl. Mater. 239 (1996) 126.

[22] K. Farrell, in: Proceedings of the Third International Workshop on Spallation Materials Technology (LANL Report: LA-UR-00-3892), Santa Fe, New Mexico, USA, April 29–May 4 (1999).
[23] G.E. Dieter, Mechanical metallurgy, 3rd Ed., McGraw-Hill, 1986, p. 283.
[24] G.R. Odette, M.Y. He, E.G. Donahue, G.E. Lucas, in: M. Sokolov, J. Landes, G. Lucas (Eds.), ASTM STP 1418, Vol. 4, America Society for Testing and Materials, West Conshohocken, PA, 2002.
[25] N. Hashimoto, these Proceedings. doi:10.1016/S0022-3115(03)00013-8.